WILEY Applied Ceramic TECHNOLOGY

Synthesis of forsterite by periclase and silica gel chlorination

Pablo Orosco[1,2] | Lucía Barbosa[1,2] | María del Carmen Ruiz[1]

[1]Instituto de Investigaciones en Tecnología Química (INTEQUI), Universidad Nacional de San Luis, San Luis, Argentina

[2]Facultad de Química, Bioquímica y Farmacia, Universidad Nacional de San Luis, San Luis, Argentina

Correspondence
Pablo Orosco
Emails: porosco@unsl.edu.ar and pablorosco@gmail.com

In this work, forsterite was synthesized by thermal treatment in chlorine of a periclase and silica gel mixture. Calcination assays were carried out in Cl_2/N_2 and air atmospheres. The effects of temperature and reaction time on the reaction of synthesis were studied. The techniques used to characterize reagents and products were thermogravimetry (TG), differential thermal analysis (DTA), X-ray diffraction (XRD), and X-ray fluorescence (XRF). The experimental results showed that pure forsterite was obtained in Cl_2/N_2 atmosphere at 700°C for 60 minutes, while in air forsterite and enstatite were partially produced at 800°C for 60 minutes.

KEYWORDS
low temperature, refractories, synthesis, thermal treatment

1 | INTRODUCTION

Forsterite is a crystalline magnesium silicate with the formula Mg_2SiO_4, which belongs to the olivine group. It has good refractoriness, low dielectric permittivity, low thermal expansion and conductivity, good chemical stability, excellent insulation properties, and good biocompatibility. These properties make forsterite an adequate material for applications as an active medium for tunable lasers and manifolds for SOFC (solid oxide fuel cells).[1-3] Recently, considerable research attention has been focused on the development of microwave telecommunication technologies because of the increased requirements for microwave applications. Forsterite is regarded as one of the most promising microwave dielectric materials.[4] Furthermore, it can be used as a biomaterial for hard tissue repair.[5,6]

The traditional forsterite synthesis method involves the reaction between MgO and SiO_2 in solid phase at high temperatures. In the last few years, several techniques have been studied for forsterite synthesis such as the alkoxy method,[7] the polymer matrix method,[8] the citrate-nitrate route,[9] the sol–gel method,[3,6,10] the combustion method,[11] the mechanothermal route,[1,5,12,13] the mechano-chemical route,[14] and high-energy ball milling.[2,4,15]

In recent studies, the pyrometallurgic process of chlorination has been successfully used to synthesize ceramic materials from the mixture of oxides or carbonate-silicates,[16-19] due to the high reactivity of the chlorinating agents and the selectivity of the chlorination reactions.

In this work, the synthesis of forsterite by the reaction between chlorine and a mixture of periclase and silica gel was investigated. The main objective was to obtain pure forsterite at low temperatures and short reaction times.

2 | MATERIALS AND METHODS

2.1 | Materials

Silica gel (SiO_2) 99%, and periclase (MgO) 99%, Sigma-Aldrich were used as the starting materials for the synthesis of forsterite. Both reagents were mixed in a disk mill for 4 minutes to get a homogeneous mixture. This mixture, denominated M, was prepared using 55% (w/w) of periclase and 45% (w/w) of silica gel in order to obtain forsterite with near-stoichiometric composition in the subsequent chlorination experiments. The XRD pattern of M shown in Figure 1 led to the identification of periclase. Silica gel phase was not detected since it has a noncrystalline form. The diffraction lines corresponding to periclase phase were simulated by using the software DF 200-DA IMAGES.[20] The results obtained show that diffraction lines correlate with the experimental peaks.

The gasses used in the different assays were 99.5% chlorine, Cofil, Argentina, 99.99% nitrogen and 99.99% chromatographic air, Air Liquide, Argentina. It is worth mentioning that nitrogen gas was used to dilute chlorine during the chlorination assays.

2.2 | Equipment

The experimental chlorination assays were performed in a thermogravimetric system designed in our laboratory.[21] The device is provided with a quartz reactor inside an electronic furnace equipped with a temperature controller. The temperature was measured with a chromel-alumel thermocouple with an accuracy of ± 5 K. The mass measurement system was an analytical balance (Mettler Toledo AB204-S/FACT, maximum sensitivity of 0.0001 g) connected to an automatic data logger.

The chemical composition of the periclase-silica gel mixture and reaction products of the different assays were determined by XRF with an X-ray fluorescence spectrometer (Philips PW 1400). The crystalline phases contained in the mixture and the reaction products were identified by XRD with an X-ray diffractometer (Rigaku D-Max-IIIC), operated at 35 kV, 30 mA.

The phenomena that occurred during the calcination of the mixture in air were studied by DTA using a thermal analyzer (Shimadzu DTG-60).

2.3 | Procedure

Isothermal and nonisothermal calcination assays were carried out in air and Cl_2/N_2 (50% v/v). For the different thermal treatments, masses of approximately 0.5 g and flows of 50 mL min^{-1} of air and 100 mL min^{-1} of Cl_2/N_2 were used. In each nonisothermal experiment, the sample was calcined in either air or Cl_2/N_2 mixture at a heating rate of 5°C min^{-1} until a temperature of 900°C was reached. The mass change was recorded as a function of temperature. The isothermal trials in air were performed roasting the sample at a heating rate of 5°C min^{-1}. Upon attainment of the working temperature, the sample was kept in air for 15 min. Then, the sample was cooled down and analyzed by XRD.

For chlorination isothermal assays, the sample was calcined in N_2 at a heating rate of 5°C min^{-1}, until the working temperature was reached. Once the temperature was stable, chlorine was fed into the reactor, generating the Cl_2/N_2 mixture (50% v/v). The sample was kept at this temperature for 15 minutes. When the reaction time was over, chlorine supply was cut off, and the sample was cooled down. The chlorinated residues obtained were analyzed by XRF. Subsequently, these residues were subjected to processes of washing and filtration with the purpose of removing the magnesium chloride generated during the chlorination. Finally, the resultant wet residues were dried in an oven at 100°C. In some cases, the filtering liquid evaporated in an oven at 100°C. The washed and dried residues were analyzed by XRD. Periclase and forsterite phases identified in XRD patterns of the residues calcined in air and Cl_2/N_2 were simulated by software DF 200-DA IMAGES.

Isothermal assays were performed in both air and Cl_2/N_2 mixture in the temperature interval ranging from 600 to 900°C for periods of 15 minutes. These experiments were carried out with the purpose of clarifying the phenomena taking place during the calcination of M in both atmospheres.

3 | RESULTS AND DISCUSSION

3.1 | Calcination in air

The calcination experiments in air were carried out in order to determine the phenomena occurring during thermal treatment of periclase-silica gel mixture in this atmosphere. The results of thermogravimetric, differential thermal, and X-ray diffraction analyses of M in air are presented in Figures 2 and 3.

The DTA curve showed an endothermic peak at around 70°C and an exothermic peak at about 800°C. These peaks corresponded to two different processes: the removing of water physically adsorbed in the sample and the synthesis of both forsterite and enstatite, respectively. The TG curve exhibited a mass loss zone between 20 and 210°C. This
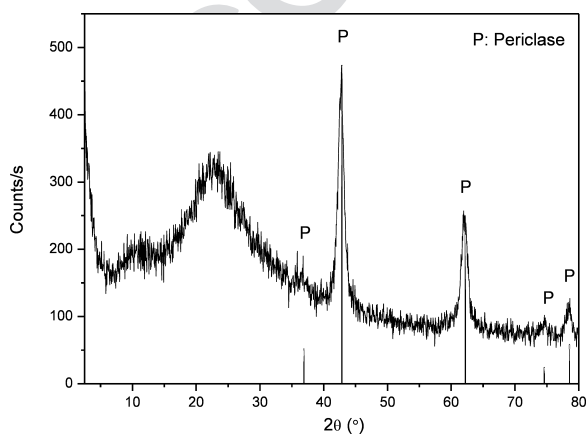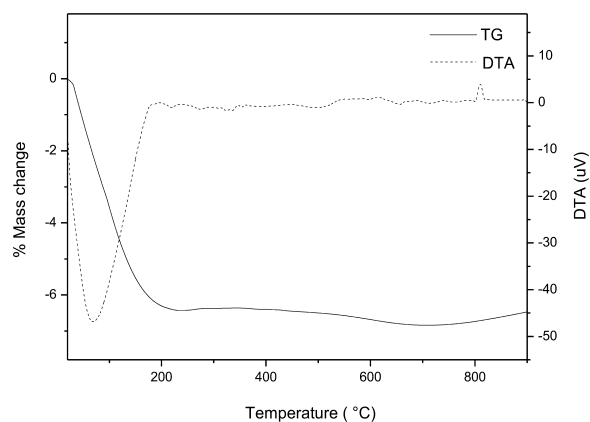

FIGURE 1 XRD pattern of the M sample

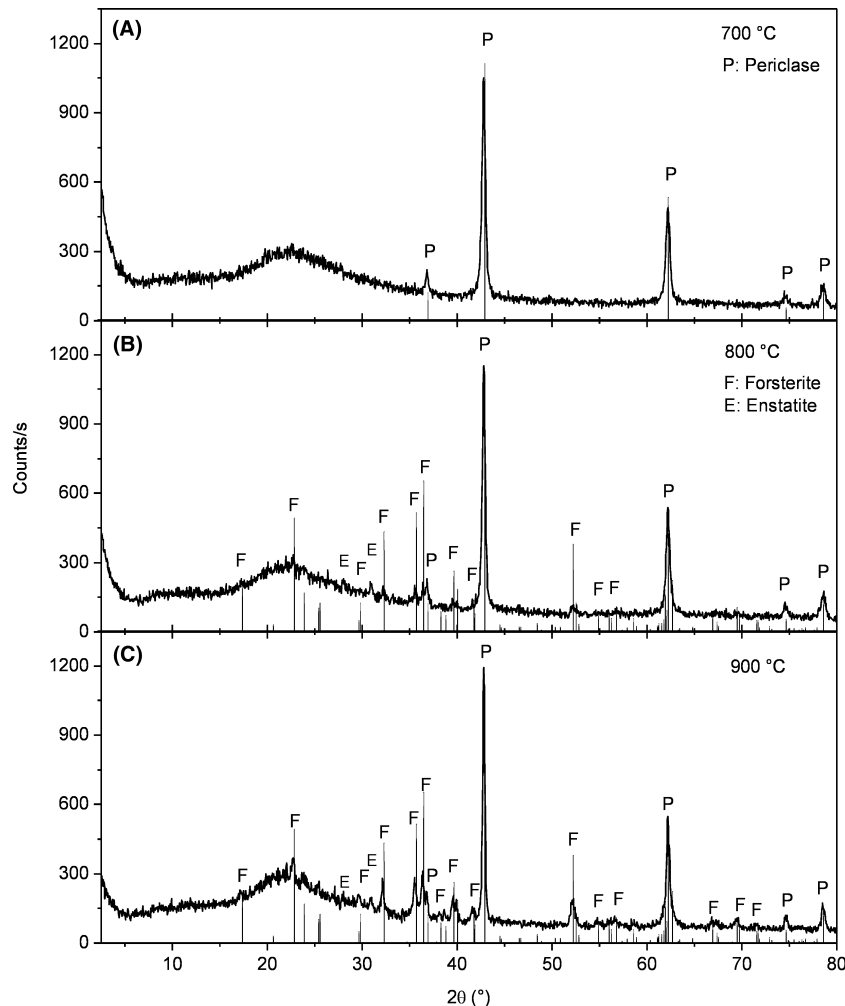**FIGURE 2** TG and DTA curves of M calcined in air

FIGURE 3   XRD patterns corresponding to M calcined in air at: (A) 700°C for 15 minutes, (B) 800°C for 15 minutes, and (C) 900°C for 15 minutes

region is related to the dehydration of the mixture. The detection of forsterite and enstatite in the diffraction pattern of the sample chlorinated at 800°C (Figure 3B) confirms the DTA results.

Figure 3C corresponds to the sample calcined at 900°C and shows an increase in the peak intensity of forsterite in comparison with the sample calcined at 800°C (Figure 3B). This fact indicated that the crystallization of forsterite continued up to the investigated temperature.

3.2 │ Calcination in Cl_2/N_2 atmosphere

The chlorination assays were carried out with the aim of determining the influence of chlorine on the synthesis of forsterite.

Figure 4 shows the thermogravimetric results of the nonisothermal treatment of M in Cl_2/N_2 current.

The thermogravimetric curve exhibited two zones of mass gain and three zones of mass loss. The first region was observed in the temperature range between 20 and 80°C and it was associated with a mass gain of 0.1%. The second region was observed in the temperature interval between 80 and 220°C, and corresponds to a mass loss of 0.1%. The third region occurred between 660 and 760°C and it is related with a mass gain of 0.7%. The fourth region was observed between 760 and 850°C and with a
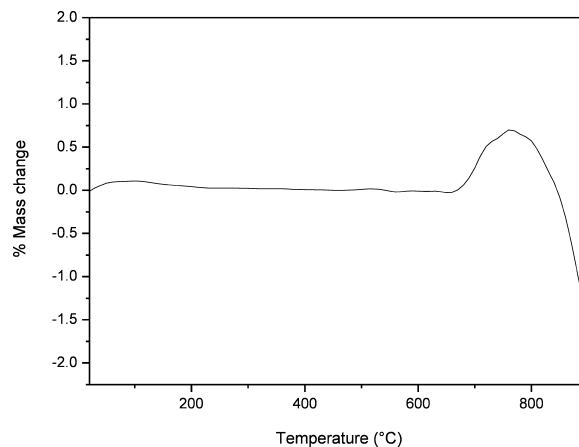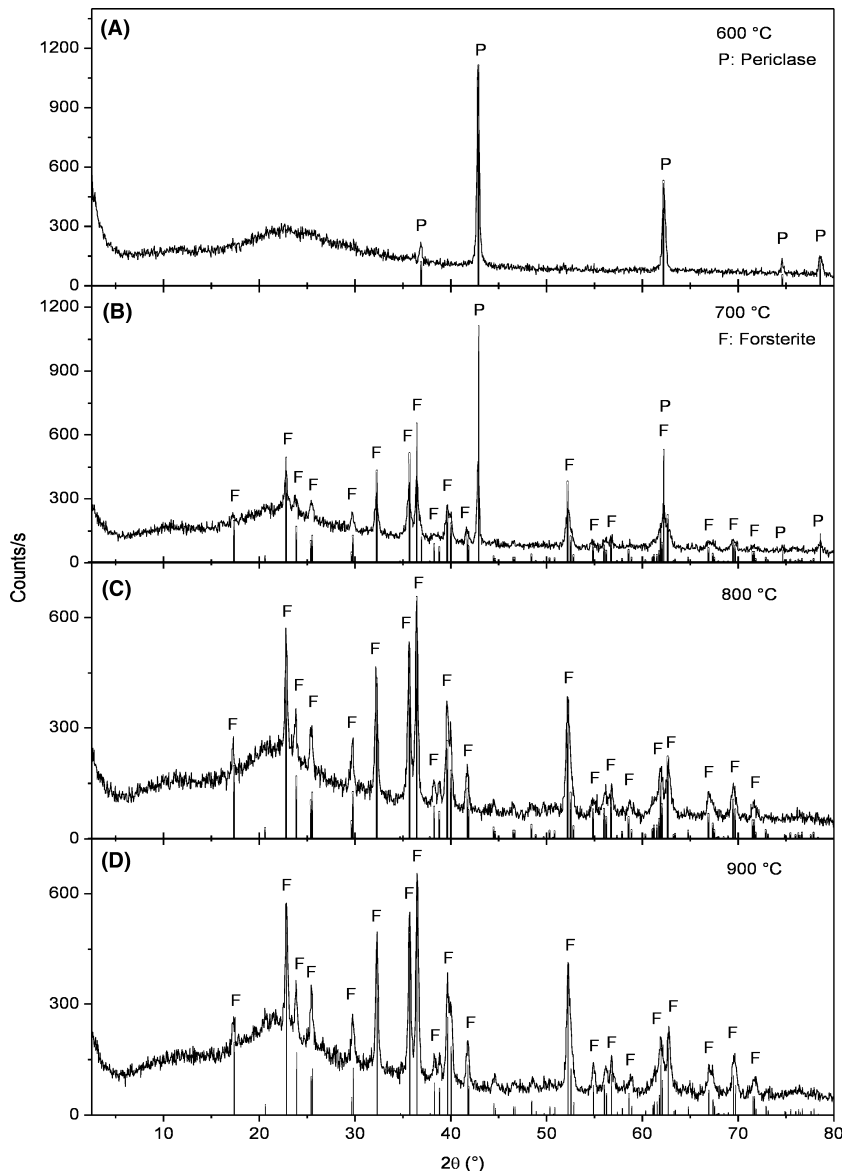

FIGURE 4   TG curve of M calcined in Cl_2/N_2

FIGURE 5 XRD patterns corresponding to M calcined in Cl_2/N_2 at: (A) 600°C for 15 minutes, (B) 700°C for 15 minutes, (C) 800°C for 15 minutes, and (D) 900°C for 15 minutes

percentage of mass loss of 0.7%. The last region, between 850 and 900°C, corresponded to a mass loss of 1.6%.

The phenomena that produce these mass changes were investigated by XRD.

The diffractograms of chlorination residues obtained at different temperatures for 15 min are presented in Figure 5.

3.2.1 | First and second zones of mass change (20-80°C and 80-220°C)

The mass changes observed in these temperature intervals (Figure 4) were a result of a balance between a mass gain produced by the adsorption of chlorine on sample and a mass loss produced by the dehydration of the sample.
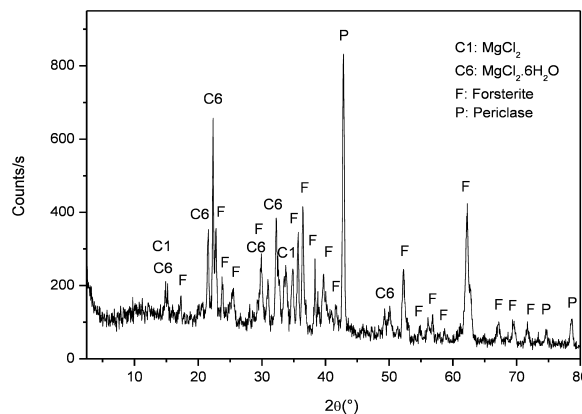
FIGURE 6 XRD pattern corresponding to M calcined in Cl_2/N_2 at 700°C for 10 minutes

TABLE 1 Contents of magnesium and silica, expressed as MgO and SiO_2, in the chlorination residues of M at different temperatures and periods of 15 minutes (determined by XRF)

Temperature (°C)	MgO (%w/w)	SiO_2 (%w/w)
600	54.56	45.42
700	54.41	45.31
850	54.52	45.44
900	53.72	46.27

3.2.2 | Third and four zones of mass change (660-760°C and 760-850°C)

The mass changes produced in these two regions corresponded to a balance between mass gain and loss occurring in the sample as a consequence of the phenomena taking place in each temperature interval.

The XRD patterns shown in Figure 5 allowed to infer the occurrence of the following events in the two mass change zones:
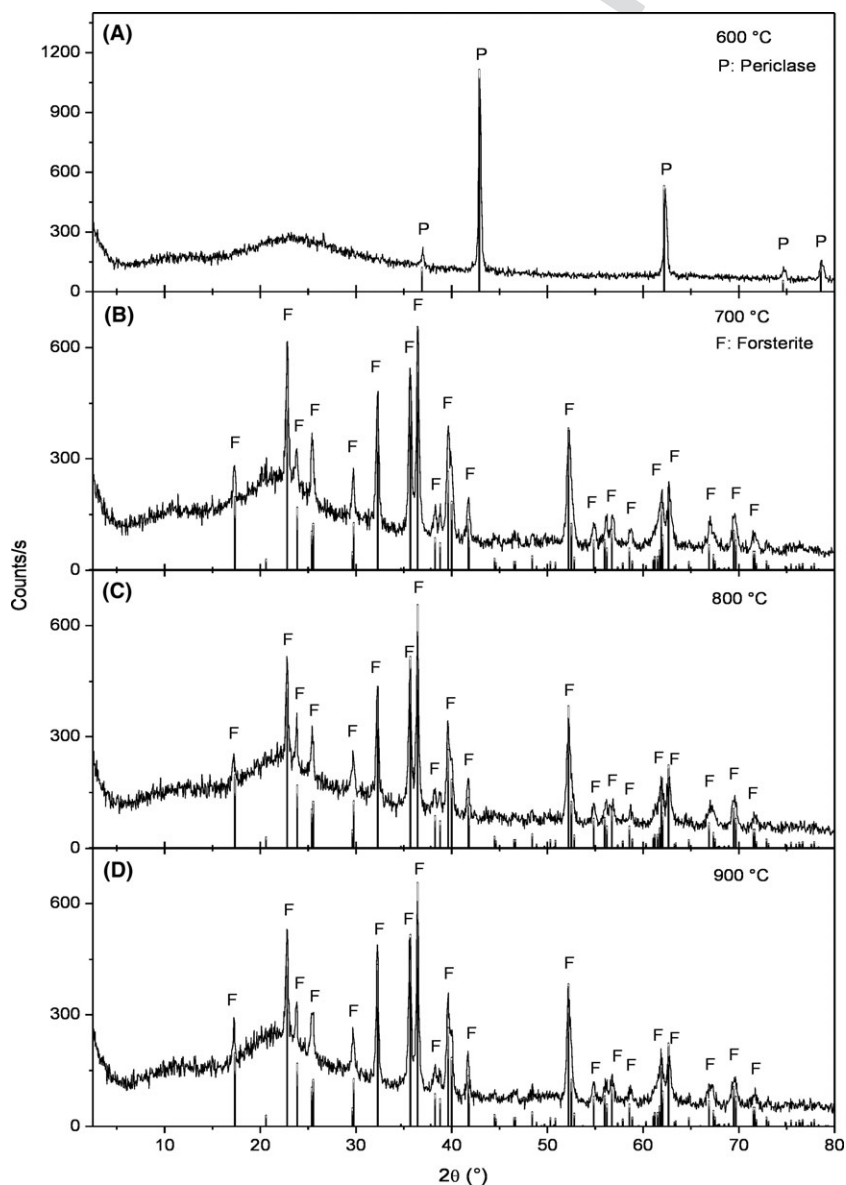
Step 1. Chlorination of periclase
Periclase reacted with chlorine to form magnesium chloride and $O_2(g)$ as follows:

$$MgO + Cl_2(g) \rightarrow MgCl_2 + 1/2O_2(g) \qquad (1)$$
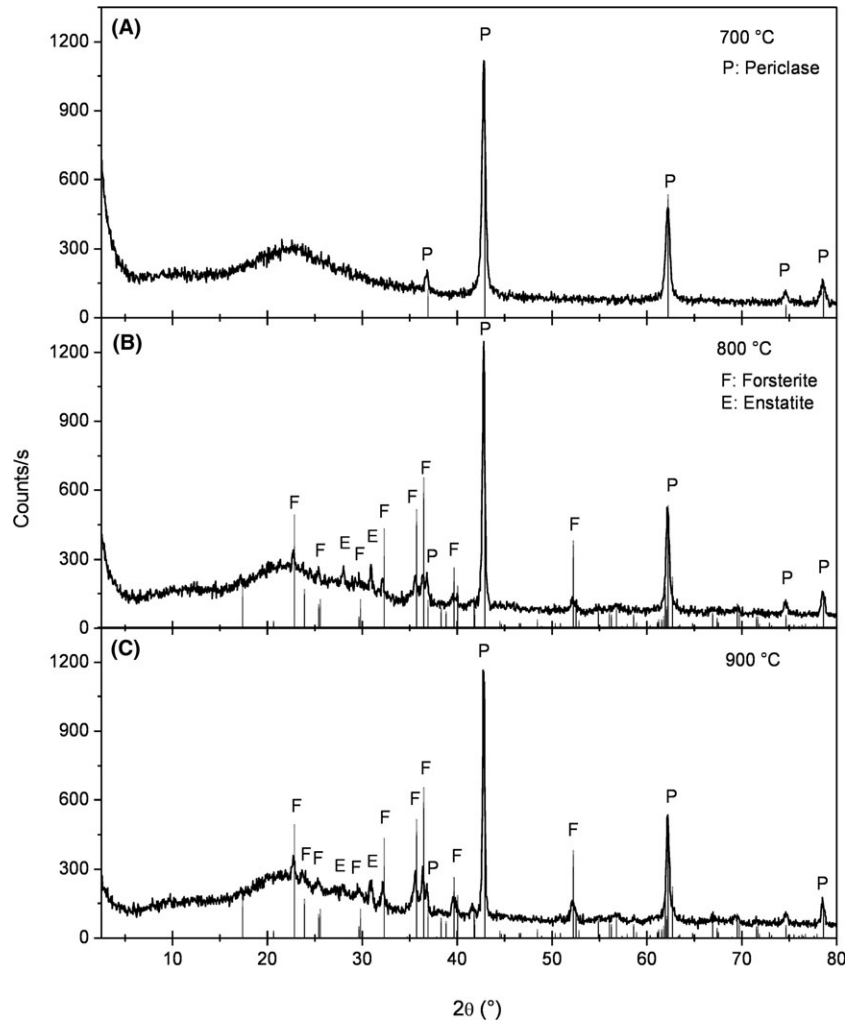
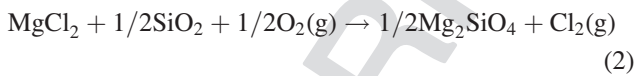### Step 2. Forsterite synthesis
Magnesium chloride and $O_2(g)$ produced by periclase chlorination reacted with silica gel at 700°C and generated forsterite, according to reaction (2):

FIGURE 7 XRD patterns corresponding to M calcined in Cl_2/N_2 at: (A) 600°C for 60 minutes, (B) 700°C for 60 minutes, (C) 800°C for 60 minutes, and (D) 900°C for 60 minutes

FIGURE 8 XRD patterns corresponding to M calcined in air at: (A) 700°C for 60 minutes, (B) 800°C for 60 minutes, and (C) 900°C for 60 minutes

$$MgCl_2 + 1/2SiO_2 + 1/2O_2(g) \rightarrow 1/2Mg_2SiO_4 + Cl_2(g) \tag{2}$$

This proposed reaction mechanism for forsterite synthesis was experimentally verified by performing an additional experiment, which consisted in the calcination of M at 700°C for 10 minutes in a Cl_2/N_2 mixture (50% v/v). Subsequently, the residual sample was analyzed by XRD and the result is shown in Figure 6. It indicates the presence of periclase, $MgCl_2$, and forsterite phases, which confirms the occurrence of reactions (1) and (2). The presence of chlorine prevents magnesium chloride from being transformed into periclase. [19] The mass changes observed in the third and fourth zones between 660 and 760°C and between 760 and 850°C, respectively, were a result of the prevalence of a phenomenon over the other. On one hand, the chlorination of periclase caused a mass gain in the sample due to the incorporation of chlorine as $MgCl_2$ (reaction (1)). On the other hand, forsterite generation (reaction (2)) produced a mass loss as a consequence of the elimination of chlorine.

3.2.3 | Sixth zone of mass change (850-900°C)

Forsterite started to be chlorinated at temperatures above 850°C, generating $MgCl_2(g)$, vitreous silica, and $O_2(g)$, according to following reaction:

$$1/2Mg_2SiO_4 + Cl_2(g) \rightarrow MgCl_2(g) + 1/2SiO_2 + 1/2O_2(g) \tag{3}$$
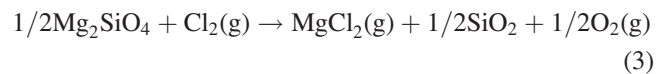
Forsterite chlorination occurred as a result of partial volatilization of $MgCl_2$. This chloride can volatilize at this temperature since it has a vapor pressure of 0.023 atm.[21] Volatile $MgCl_2$ was entrained by the gaseous stream of Cl_2/N_2, leaving the reaction zone, thus favoring the reaction of formation of more $MgCl_2(g)$.

The formation of volatile $MgCl_2$ can be observed in Figure 4 as the mass loss from 850 to 900°C.

The results of the XRF analysis corroborated the phenomena taking place in the last three zones of mass change. The concentrations of Mg and Si present in the

chlorination residues obtained at different temperatures and a reaction time of 15 minutes are presented in Table 1.

Forsterite chlorination was confirmed by the results obtained by XRF at 900°C, which indicated a decrease in Mg concentration as a consequence of removing volatile $MgCl_2$ generated by reaction (3).

3.3 | Optimal conditions for forsterite synthesis

With the purpose of determining which conditions are the optimal for forsterite formation, isothermal assays in Cl_2/N_2 flow were carried out in the temperature interval between 600 and 900°C for 60 minutes. The residues of these trials were analyzed by XRD and the results are shown in Figure 7. The phases identified as periclase and forsterite in the XRD patterns were simulated. The comparison between simulation results and experimental data revealed that the simulated lines correlate with the peaks corresponding to the phases identified as periclase and forsterite.

In addition, isothermal calcination assays in air were performed between 700 and 900°C for 60 minutes to draw a comparison with the calcination assays in Cl_2/N_2. XRD patterns of calcination residues in air are presented in Figure 8.

XRD patterns shown in Figures 7 and 8 indicated that the thermal treatment of periclase-silica gel mixture in Cl_2/N_2 atmosphere produced forsterite in the temperature interval between 700 and 900°C. Forsterite was partially generated between 800 and 900°C in air; further, enstatite was produced in such conditions.

By comparing the XRD patterns corresponding to the residues calcined in Cl_2/N_2 at different temperatures for 15 and 60 minutes, it can be inferred that forsterite was partially produced at 700°C for 15 minutes, since periclase was not totally consumed in reaction (2) (Figure 5B). The periclase phase disappeared at 700°C and a reaction time of 60 minutes, which indicates that forsterite formation was completed (Figure 7B). Furthermore, under these conditions, $MgCl_2$ did not crystallize by the evaporation of the filtering liquid obtained by washing the chlorination residue. This fact indicates that magnesium chloride was totally consumed in reaction (2).

The comparison between the XRD patterns of the residues chlorinated at 800°C for 15 and 60 minutes shows that the peak intensities corresponding to forsterite are similar. However, the thermogram of M calcined in Cl_2/N_2 (Figure 4) showed a mass gain at 800°C, which indicates that forsterite formation is still incomplete at 15 minutes.

Although XRD patterns of Figures 5C, D and 7C, D are similar, the mass loss observed from 850 to 900°C in

the thermogram corresponding to M (Figure 4) shows that forsterite chlorination was produced. According to these results, it can be inferred that forsterite chlorination occurred at 900°C and reaction times of 15 and 60 minutes. Our results show that the optimal conditions to produce forsterite are 700°C and reaction time of 60 minutes.

Purity of forsterite was determined applying the RIR (reference intensity ratio) method with the diffraction data of the chlorination residue of M at 700°C for 60 minutes. The results indicated that the purity of forsterite is 100%, which was confirmed by the absence of a crystallized solid
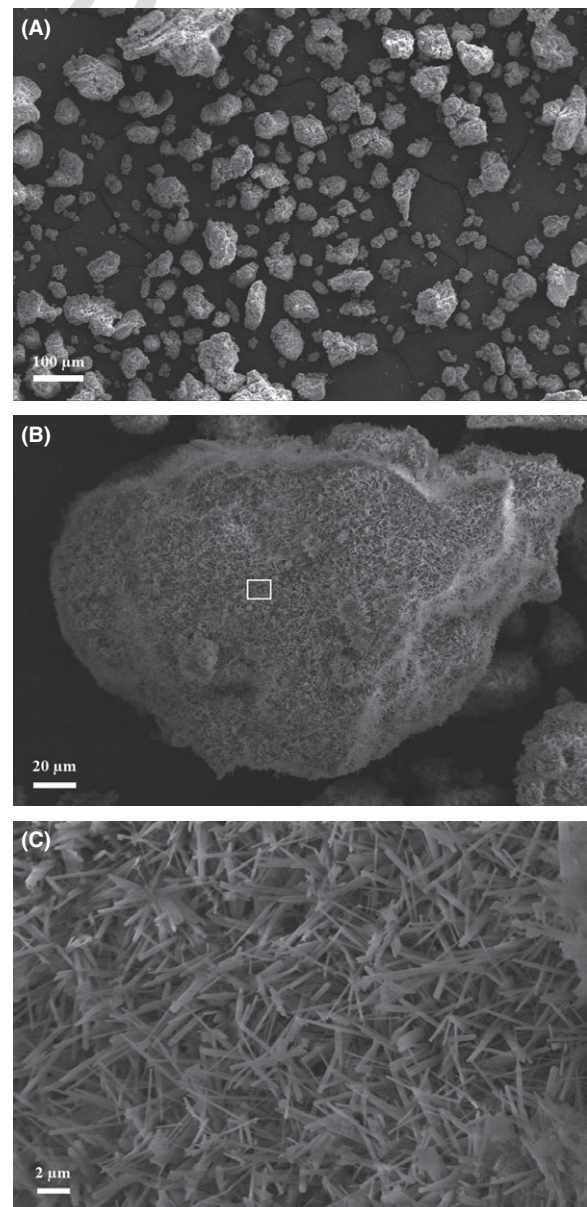
FIGURE 9 SEM micrographs corresponding to M sample calcined in Cl_2/N_2 at 800°C and 60 minutes: (A) overall view, (B) morphology of an agglomerate of particles, and (C) amplified image of the particles marked in (B)

after the evaporation of the filtering liquid obtained by washing of the chlorination residue.

3.3.1 | SEM analysis

SEM images of the forsterite synthesized by chlorination of M at 800°C and a reaction time of 60 minutes are presented in Figure 9. It can be seen from Figure 9A that forsterite is made up of agglomerates of particles with different sizes and irregular shapes. SEM image of an agglomerate shows that it is made up of particles with uniform size and regular shape (Figure 9B). An amplified image of the agglomerate of particles shown in Figure 9B reveals that the particles of forsterite have needle shape (Figure 9C).

4 | CONCLUSION

The experimental results show that the pyrometallurgic process of chlorination is an efficient method to obtain forsterite at low temperatures and short reaction times. A single phase forsterite was generated by chlorination of a periclase and silica gel mixture with a periclase/silica gel molar ratio of 2:1 at 700°C and a reaction time of 60 minutes, while during calcination of M in air at 800°C for 60 minutes, enstatite and forsterite phases were partially produced.

It was observed that forsterite formation is absolutely selective between 700 and 850°C for periods of 60 minutes.

In the assayed system, forsterite synthesis occurs through the following steps: the chlorination of periclase that generates $MgCl_2$, and the subsequent reaction of $MgCl_2$ with silica gel that produces forsterite.

The optimal conditions to produce forsterite are 700°C and reaction time of 60 minutes, since under these conditions the forsterite synthesis reaction is complete.

REFERENCES

1. Tavangarian F, Emadi R. Synthesis of nanocrystalline forsterite (Mg_2SiO_4) powder by combined mechanical activation and thermal. *Mater Res Bull*. 2010;45:388–391.

2. Barzegar Bafrooei H, Ebadzadeh T, Majidian H. Microwave synthesis and sintering of forsterite nanopowder produced by high energy ball. *Ceram Int*. 2014;40:2869–2876.

3. Hadri ME, Ahamdane H, El Idrissi Raghni MA. Sol gel synthesis of forsterite, M–doped forsterite (M = Ni, Co) solid solutions and their use as ceramic pigments. *J Eur Ceram Soc* 2015;35:765–777.

4. Cheng L, Liu P, Chen X, et al. Fabrication of nanopowders by high energy ball milling and low temperature sintering of Mg_2SiO_4 microwave dielectrics. *J Alloy Compd*. 2012;513:373–377.

5. Ghomi H, Jaberzadeh M, Fathi MH. Novel fabrication of forsterite scaffold with improved mechanical properties. *J Alloy Compd*. 2011;509:L63–L68.

6. Hassanzadeh–Tabrizi A, Bigham A, Rafienia M. Surfactant–assisted sol–gel synthesis of forsterite nanoparticles as a novel drug delivery system. *Mater Sci Eng, C* 2016;58:737–741.

7. Yamaguchi O, Nakajima Y, Shimizu K. Formation of forsterite (2MgO SiO₂) from the mixture prepared by alkoxy–method. *Chem Lett* 1976;5:401–404.

8. Saberi A, Alinejad B, Negahdari Z, Kazemi F, Almasi A. A novel method to low temperature synthesis of nanocrystalline forsterite. *Mater Res Bull*. 2007;42:666–673.

9. Saberi A, Negahdari Z, Alinejad B, Golestani-Fard F. Synthesis and characterization of nanocrystalline forsterite through citrate–nitrate route. *Ceram Int*. 2009;35:1705–1708.

10. Sanosh KP, Balakrishnan A, Francis L, Kim TN. Sol–gel synthesis of forsterite nanopowders with narrow particle size. *J Alloy Compd*. 2010;495:113–115.

11. Mostafavi K, Ghahari M, Baghshahi S, Arabi AM. Synthesis of Mg_2SiO_4: Eu^{3+} by combustion method and investigating its luminescence properties. *J Alloy Compd*. 2013;555:62–67.

12. Chen L, Ye G, Zhou W, et al. Influence of MgO precursors on mechanically activated forsterite synthesis. *Ceram Int*. 2015;41:12651–12657.

13. Tavangarian F, Emadi R. Mechanical activation assisted synthesis of pure nanocrystalline forsterite powder. *J Alloy Compd*. 2009;485:648–652.

14. Fathi MH, Kharaziha M. The effect of fluorine ion on fabrication of nanostructure forsterite during mechanochemical synthesis. *J Alloy Compd*. 2009;472:540–545.

15. Kosanović C, Stubičar N, Tomašić N, Bermanec V, Stubičar M. Synthesis of a forsterite powder by combined ball milling and thermal treatment. *J Alloy Compd*. 2005;389:306–309.

16. Orosco P, Barbosa L, del Carmen Ruiz M. Synthesis of magnesium aluminate spinel by periclase and alumina chlorination. *Mater Res Bull* 2014;59:337–340.

17. Orosco P, del Carmen Ruiz M, González J. Phase transformations of a talc ore under heated chlorine atmosphere. *Thermochim Acta* 2013;554:15–24.

18. Orosco P, del Carmen Ruiz M, González J. Synthesis of cordierite by dolomite and kaolinitic clay chlorination. Study of the phase transformations and reaction mechanism. *Powder Technol* 2014;267:111–118.

19. Orosco P, del Carmen Ruiz M. Potassium chloride production by microcline chlorination. *Thermochim Acta* 2015;613:108–112.

20. DF 200-DA IMAGES, 1993. Rigaku, Austin, United States.

21. Túnez FM, González J, del Carmen Ruiz M Aparato de Laboratorio para Realizar Termogravimetrías en Atmósferas Corrosivas y no Corrosivas. Patent P060100450, 2007.

22. HSC Chemistry for Windows Software V. 5.1, 2003. Outokumpu Research, Pori, Finland.